AGU PUBLICATIONS

JGR

Journal of Geophysical Research: Earth Surface

RESEARCH ARTICLE

10.1002/2016JF004071

Key Points:
- Longitudinal surface structures are often used to inform about past configurations of ice sheets, but their formation is debated
- Analysis of the morphological and glaciological properties of >40,000 longitudinal surface structures across Antarctica
- We propose that longitudinal surface structures are the consequence of increased strain encountered by ice in four flow configurations

Supporting Information:
- Supporting Information S1

Correspondence to:
J. C. Ely,
j.ely@shef.ac.uk

Citation:
Ely, J. C., C. D. Clark, F. S. L. Ng, and M. Spagnolo (2017), Insights on the formation of longitudinal surface structures on ice sheets from analysis of their spacing, spatial distribution, and relationship to ice thickness and flow, *J. Geophys. Res. Earth Surf.*, *122*, 961–972, doi:10.1002/2016JF004071.

Received 31 AUG 2016
Accepted 28 MAR 2017
Accepted article online 31 MAR 2017
Published online 20 APR 2017

Insights on the formation of longitudinal surface structures on ice sheets from analysis of their spacing, spatial distribution, and relationship to ice thickness and flow

J. C. Ely[1], C. D. Clark[1], F. S. L. Ng[1], and M. Spagnolo[2,3]

[1]Department of Geography, University of Sheffield, Sheffield, UK, [2]Department of Geography and Environment, School of Geosciences, University of Aberdeen, Aberdeen, UK, [3]Department of Earth and Planetary Science, University of California, Berkeley, California, USA

Abstract Longitudinal surface structures (LSSs) are prevalent upon the ice streams, ice shelves, and outlet glaciers of ice sheets. These features inform our understanding of past and present ice sheet behavior. However, consensus regarding their genesis has not been reached. Here we analyze 42,311 LSS segments mapped across Antarctica together with geophysical data to determine their morphological and glaciological properties. Most LSSs are spaced 450 to 1500 m apart, a distance positively correlated with the width of the ice flow unit on which they occur. The start points (upstream end locations) of LSSs have diverse ice thicknesses and velocities. The majority of LSSs occur where ice flow is converging or broadly parallel, and they are prominent at ice confluences. Some occur at slow-flowing ice stream onsets. Occasionally, LSSs relate to sudden variations in basal shear stress due to basal perturbations. From these observations, we argue that LSSs are the consequence of increased strain which occurs during the lateral compression and longitudinal extension of ice: (i) converging/flowing into a channel (this scenario characterizes most LSSs), (ii) at the onset of ice streaming, (iii) at flow unit confluence, and (iv) as ice flows over and around a basal perturbation.

1. Introduction

Flow-parallel curvilineations are pervasive on the surface of ice streams, ice shelves, and outlet glaciers. They are especially numerous on the Antarctic Ice Sheet [*Crabtree and Doake*, 1980; *Dowdeswell and McIntyre*, 1987; *Ely and Clark*, 2016] and have been observed on the surface of the Greenland Ice Sheet [*Joughin et al.*, 1999; *Mayer and Herzfeld*, 2000; *Jezek et al.*, 2013] and other large ice masses [*Burgess et al.*, 2005; *Wyatt and Sharp*, 2015]. These longitudinal surface structures (LSSs, Figure 1), also known as flowstripes [*Casassa*, 1991], longitudinal foliations [*Reynolds and Hambrey*, 1988], streaklines [*Raup et al.*, 2005], flow bands [*Swithinbank et al.*, 1988], or flow lines [*Crabtree and Doake*, 1980], can stretch for hundreds of kilometers [*Glasser and Scambos*, 2008; *Glasser et al.*, 2015] and endure for centuries on the ice surface [*Casassa and Whillans*, 1994; *Gudmundsson et al.*, 1998]. Their ubiquity and persistence means that they can be compared to modern-day surface velocity fields [e.g., *Rignot et al.*, 2011] in order to distinguish regions where ice flow direction has changed [*Fahnestock et al.*, 2000; *Conway et al.*, 2002; *Catania et al.*, 2012] from regions where the flow configuration has remained consistent [*Glasser et al.*, 2015]. However, the precise mechanism(s) behind the formation of LSSs is unresolved. This knowledge gap limits their utility for deciphering glacial processes and history.

A plethora of mechanisms have been invoked to account for LSS formation (see *Glasser and Gudmundsson* [2012] for a review), of which the lateral compression and longitudinal extension hypothesis and the basal transfer hypothesis are the most frequently discussed. The first regards LSSs as the product of lateral compression and longitudinal extension as ice converges into a channel or trunk [*Reynolds and Hambrey*, 1988; *Hambrey and Dowdeswell*, 1994; *Glasser et al.*, 2015], making LSSs larger equivalents of the longitudinal foliations (from internal folding) observed on valley glaciers [e.g., *Hambrey and Milnes*, 1977; *Jennings et al.*, 2014]. Additionally, LSSs often originate at confluences of ice tributaries [*Swithinbank and Lucchitta*, 1986; *Vornberger and Whillans*, 1986], where strong lateral compression and longitudinal extension are thought to cause "trough-like" depressions in the ice surface [*Glasser and Gudmundsson*, 2012]. The second main formation hypothesis (the basal transfer hypothesis) attributes LSSs to ice flow over an uneven bed [*Hodge and Doppelhammer*, 1996; *Gudmundsson et al.*, 1998]. Here irregularities in basal topography (i.e., subglacial hills)

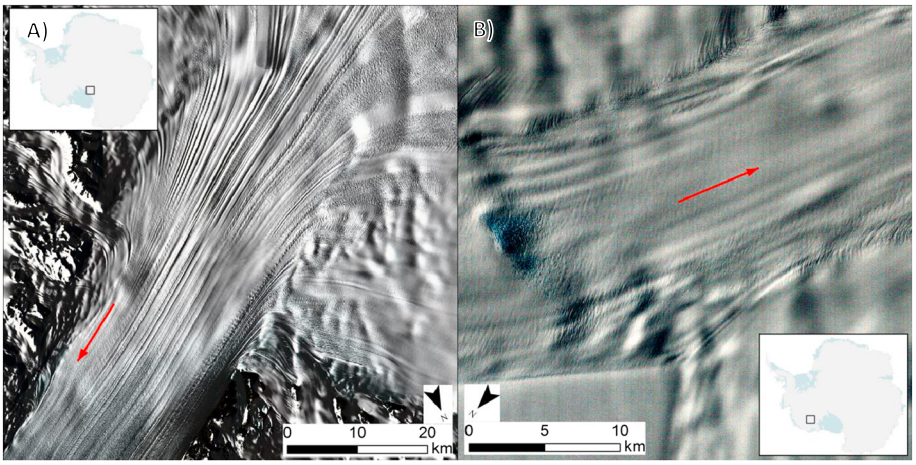

Figure 1. Landsat imagery of LSSs on the surface of (a) Byrd glacier and (b) MacAyeal ice stream, in Antarctica. Red arrows indicate approximate ice flow direction.

or basal shear stress (i.e., sticky spots) that are comparable in wavelength to the ice thickness cause a surface perturbation which is then elongated down ice flow to form an LSS. This process becomes effective where basal sliding dominates over internal deformation in contributing to ice flow velocity [*Gudmundsson et al*., 1998]. Which of these two hypotheses validly explains the global population of LSSs, or whether both are pertinent, is not known. It is even unclear whether LSSs are a single phenomenon requiring one explanation or if multiple mechanisms are required. If the latter, the conditions favoring a particular mechanism over another need to be established.

The LSS formation mechanisms outlined above have been proposed based on numerical modeling of ice flow [e.g., *Gudmundsson et al*., 1998] and qualitative observations from satellite imagery [e.g., *Merry and Whillans*, 1993; *Glasser and Gudmundsson*, 2012]. Given the availability of Pan-Antarctic satellite imagery and geophysical data sets [e.g., *Rignot et al*., 2011; *Fretwell et al*., 2014], it is now possible to analyze the morphological and glaciological properties of LSSs across the continent. Recently, *Glasser et al*. [2015] undertook extensive mapping of LSSs across Antarctica and examined their geomorphological character by studying their length and comparing their spatial distribution with bed topography and ice surface velocity. These authors conclude that LSSs predominately form by lateral compression and simple shear in converging ice flow. Here we extend this approach by using an independently derived map of Antarctic LSSs [*Ely and Clark*, 2016] and by examining more glaciological and morphological variables. For each LSS, we measure the local ice thickness, ice velocity, and planimetric ice flow convergence from a newly available data set [*Ng*, 2015]. From our mapped data set, we also derive measurements of LSS lateral spacing and LSS spatial density. The greater collection of variables allows more thorough statistical exploration that sheds further light into the formation of LSSs and offers results for testing models of LSS formation.

2. Materials and Methods

The database of LSSs analyzed here is presented as a detailed map in *Ely and Clark* [2016], along with a description of the mapping process. The mapping is redrawn at a smaller scale in Figure 2. In short, Antarctic LSSs were manually digitized using a combination of Landsat, RADARSAT, and MODIS satellite data. The mapping is comparable between data sources and independently agrees with available high-resolution lidar data [*Ely*, 2016]. The map is composed of 42,311 polylines representing LSS segments [*Ely and Clark*, 2016]. LSSs were not mapped across disruptions such as heavily crevassed regions or surface mottling, in order to avoid extrapolation or ambiguity. Therefore, the mapping likely underrepresents the true distribution of LSSs, due to surface disruptions or visibility issues. This limitation is taken into account later when sampling for morphological and glaciological variables. Our mapping campaign leads to a greater number of polylines generated than that of *Glasser et al*. [2015] (~ 42,000 rather than ~3600). The tenfold difference seems to stem from (i) our inclusion of the Antarctic Peninsula in our mapping (not in Glasser et al.'s data set), (ii) some operator difference in discerning LSSs, which has led to our much denser mapping of them

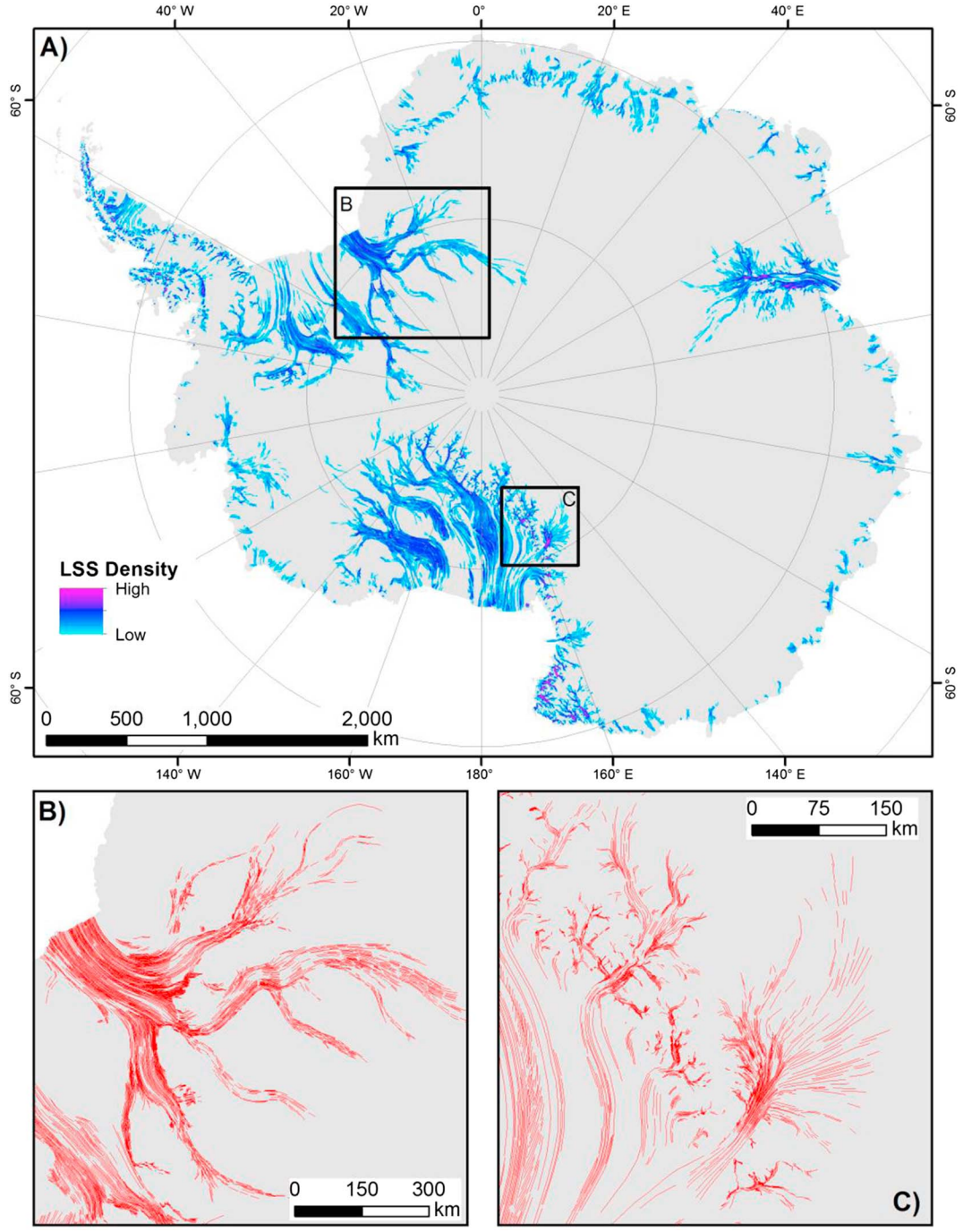

Figure 2. Overview of mapped LSSs in Antarctica. (a) The density of LSS and location of insets. (b) Mapped LSSs in the Filchner-Ronne system. (c) Mapped LSSs on glaciers in the Transantarctic Mountains. This mapping is presented in greater detail in *Ely and Clark* [2016].

in some regions (e.g., Thwaites Glacier and Queen Maud Land), and (iii) cases where *Glasser et al.* [2015] had mapped as single continuous features what we mapped as multiple features classified as disrupted LSSs (see above).

In the present study, LSSs were grouped into "flow units," regions of ice that can be traced upstream to the same source region [e.g., *Jennings et al.*, 2014]. These were defined by ice structural and textural expressions and bordered by shear margins or depressions [*Glasser and Scambos*, 2008]. LSS spacing was determined at

2027 linear transects [after *Spagnolo et al*., 2014]. These transects were placed perpendicularly to LSSs across the grounded portion of the ice sheet, with several transects per flow unit. Places where LSSs are disturbed, for example by crevasses, were avoided. Changes in the spatial frequency of LSSs along each transect were identified by first visually assessing plots of the measured spacings against the transect distance in order to evaluate changes in spatial frequency. The occurrence of either a peak or trough on these plots was recorded (see Figure S2), reflecting the concentration of LSSs at the edges or toward the center of a flow unit, respectively.

To calculate LSS density (cumulative length per unit area), the mapped LSS polylines were converted into a series of regularly spaced points, and a grid with nodes 450 m apart was constructed. This grid spacing was chosen to match velocity and convergence data [*Rignot et al*., 2011; *Ng*, 2015]. Density was defined as the total length of LSSs falling within a circular search radius from each grid node, divided by the search area. A search radius of 3 km and a point spacing of 100 m where chosen by conducting sensitivity analysis on a subset of the data covering the Lambert-Amery region, East Antarctica (supporting information S1).

Three glaciological parameters were investigated in this study: ice thickness, flow velocity, and flow convergence. They were measured for each LSS at two locations: (i) at its (upstream) start point, to characterize the environment at which LSSs begin; (ii) at the intersection between LSSs and the transects constructed to make spacing measurements, in order to elucidate any influences these parameters might have on LSS spacing. As we are concerned primarily with the formation of LSSs, this paper focusses mainly on the former location. However, when discussing the spacing of LSSs, measurements of glaciological conditions taken along spacing transects are referred to. Our ice thickness values were derived from the BEDMAP-2 compilation [*Fretwell et al*., 2014]. Ice thickness values associated with an uncertainty in bed elevation greater than 300 m were not recorded. Ice velocity was obtained from the MEaSUREs data [*Rignot et al*., 2011]. Data with an uncertainty >17 m/yr were excluded. Finally, planimetric flow convergence was obtained from the data of *Ng* [2015]. This variable quantifies the spatial rate of change of surface flow direction (θ) at any location as one "sidesteps" from it an infinitesimal distance (n) in the direction perpendicular to flow (i.e., $\mathrm{d}\theta/\mathrm{d}n$), and has values of >0, $=0$, and <0 where the ice flow is converging, parallel, and diverging, respectively. Convergence values where ice velocity is <20 m/yr are unreliable, and were therefore excluded from our analysis. Three regions of Antarctica known to exhibit relict LSSs were excluded from this parameter collection, as changes in the flow regime of the ice mean that any link between present-day ice conditions and LSS formation is likely lost. These are (i) the Bungenstock Ice Rise in the Weddell Sea sector, where LSSs are thought to show a former fast flow regime [*Siegert et al*., 2013]; (ii) the now largely inactive Kamb Ice Stream [*Catania et al*., 2005]; and (iii) the Siple Ice Stream, where LSSs reveal a former tributary of the Kamb Ice Stream [*Conway et al*., 2002].

3. Results

According to the transect measurements, LSSs are typically spaced between 450 and 1500 m apart (25th to 75th percentiles; Figures 3a and 3b), with the majority (80%) less than 1750 m apart. Although disrupted regions of LSSs were avoided during our sampling, some of the extremely large spacing values (Table 1) may be associated with regions where LSSs have been disrupted without leaving a clear surface expression. Conversely, small spacing values are likely to derive from measurements where LSSs were perceived to merge (Table 1). Such circumstances are likely exceptional, and we regard the large number of measurements (n = 14,758) and the derived medians as providing reliable average measures of LSS spacing.

The spacing of LSSs varies both within and between flow units. For the majority of transects (62%), LSSs tend to be concentrated at the flow unit lateral edges (see Figure S2). In Figures 4a and 4b the spacing measurements are grouped per flow units, revealing that the majority of flow units (83%) display a positive correlation between LSS spacing and flow unit width. Plotted together, these relationships reveal an intriguing positive correlation between mean LSS spacing and flow unit width across the measured population (Figures 4c and 4d), whose approximate linearity indicates a tendency for the number of LSSs encountered across each flow unit to be roughly similar—constrained to between 8 and 30. For a given flow unit with LSSs, a fundamental lower limit to the number of LSSs is 1 (e.g., a 3 km wide flow unit cannot have a mean LSS spacing exceeding 3 km). But it is puzzling why the observed numbers fall consistently within an order of magnitude, when our analysis includes flow units of vastly different widths. While we do not try to explain this result in this paper, it

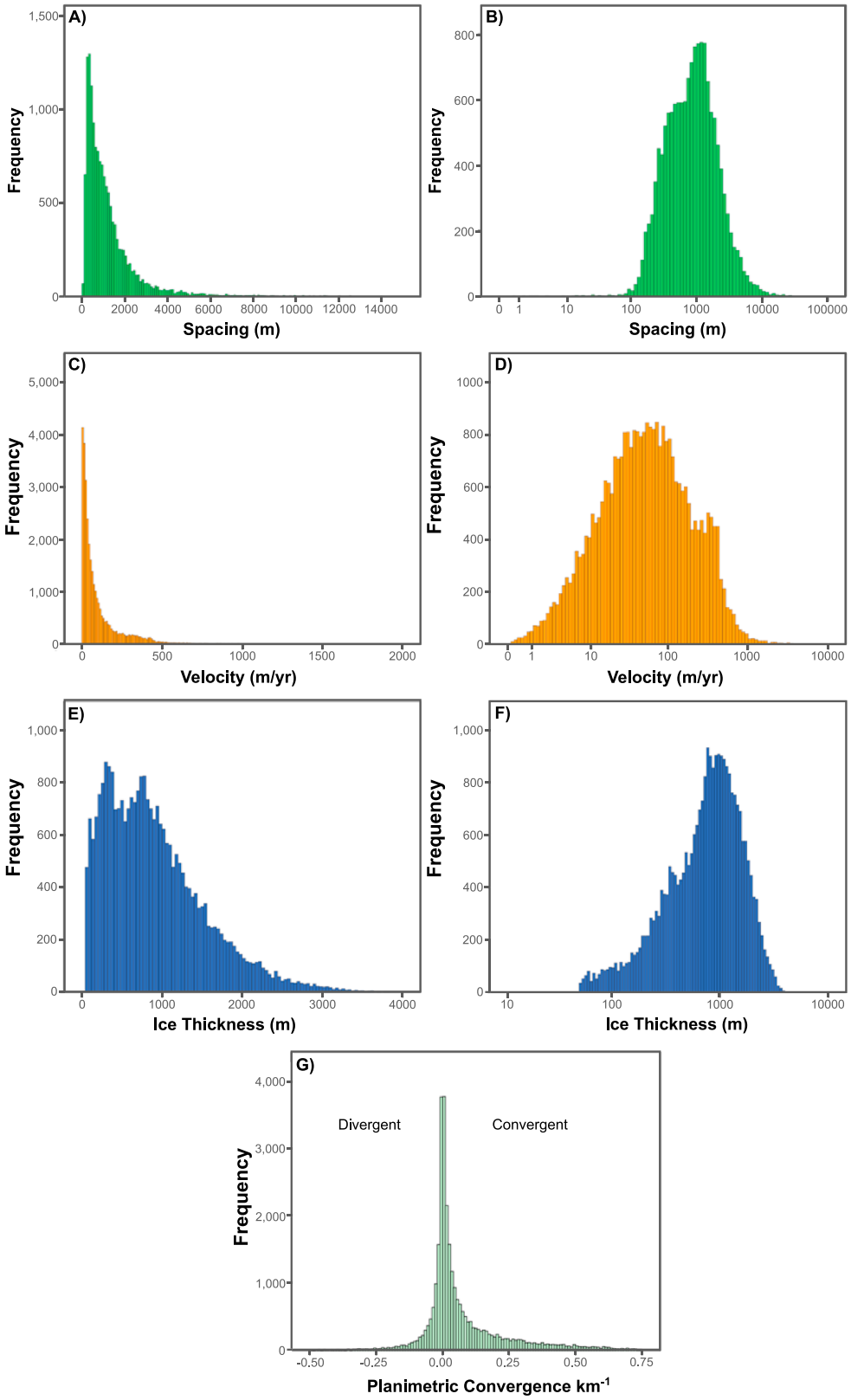

Figure 3. Spacing and glaciological properties (velocity, ice thickness, and flow convergence) of longitudinal surface structures. Data are plotted on (left column) a linear scale and (right column) a logarithmic scale; the latter scale causes a change in the data binning and therefore frequency scales. (a and b) LSSs spacing. (c and d) Ice velocity, (e and f) ice thickness, and (g) planimetric flow convergence measured from the start points of LSSs.

Table 1. Descriptive Statistics of Measured LSS Variables[a]

	Spacing (m)	Velocity (m/yr)	Thickness (m)	Planimetric Convergence (km^{-1})
Sample size (*n*)	14,758	31,148	27,656	30,252
Mean	1,240	110 (±3.2)	913 (±195)	0.79
Median	865	50.9 (±3.2)	796 (±195)	0.16
Mode	1,190	38.7 (±3.2)	341 (±195)	0.31
Skewness	5.2	5.5	1.0	0.25
Kurtosis	49.9	59.6	1.1	83.75
Minimum	0.6	0.11 (±1)	51.0 (±59)	−6.98
Maximum	28,100	3,500 (±2)	3,950 (±200)	4.48

[a]Velocity, thickness, and planimetric convergence measurements are from the LSS start point.

indicates that there is no set spacing for LSSs: Across the ice sheet, LSSs do not remain a similar distance apart regardless of ice stream width, as occurs for some subglacial bed forms such as megascale glacial lineations [e.g., *Spagnolo et al.*, 2014].

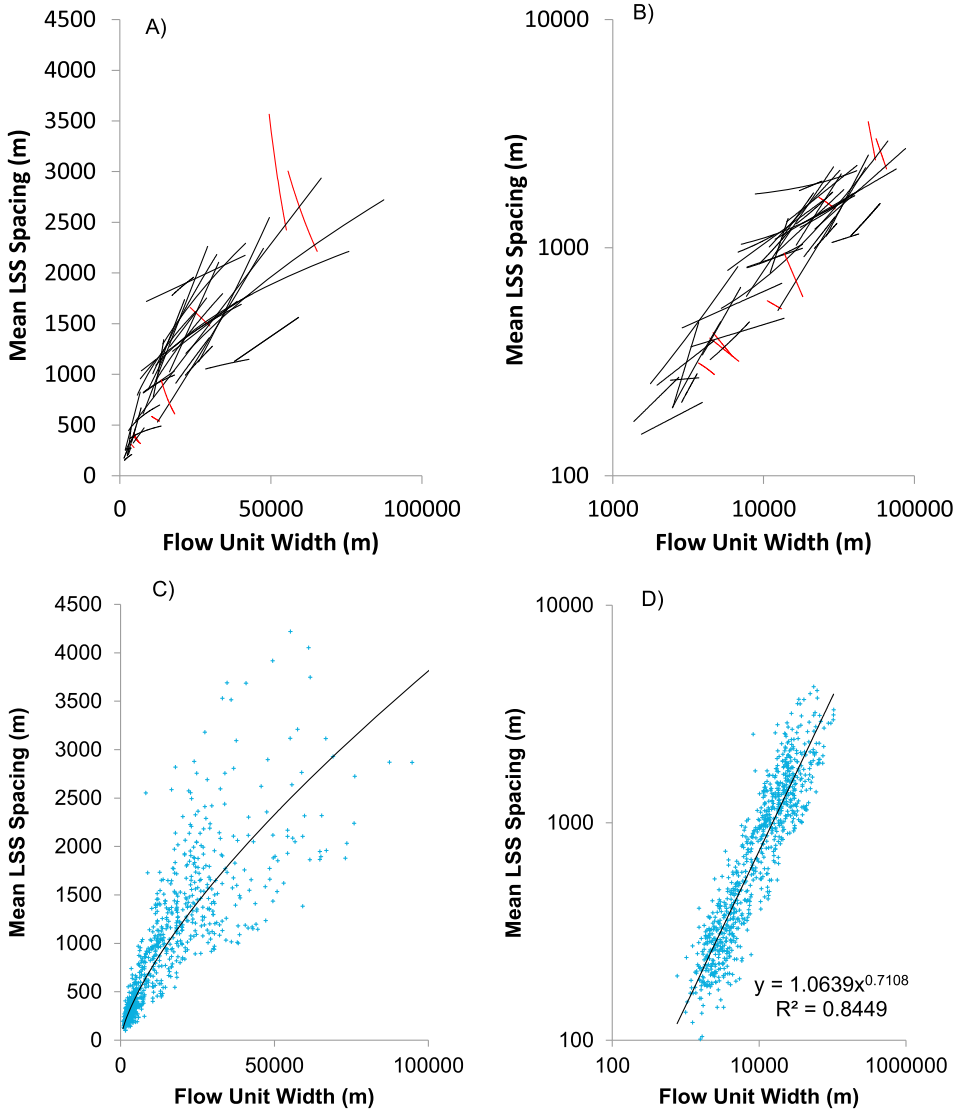

Figure 4. Strong positive relationships are found between mean LSS spacing and flow unit width. (left column) Plots on linear scales and (right column) log-log plots. (a and b) The "local" regression lines when transects are grouped according to their flow units. The majority are positive correlations (black). Negative correlations are plotted in red. (c and d) An overall positive correlation between flow unit width and LSS spacing. All relationships plotted are significant ($p = <0.05$).

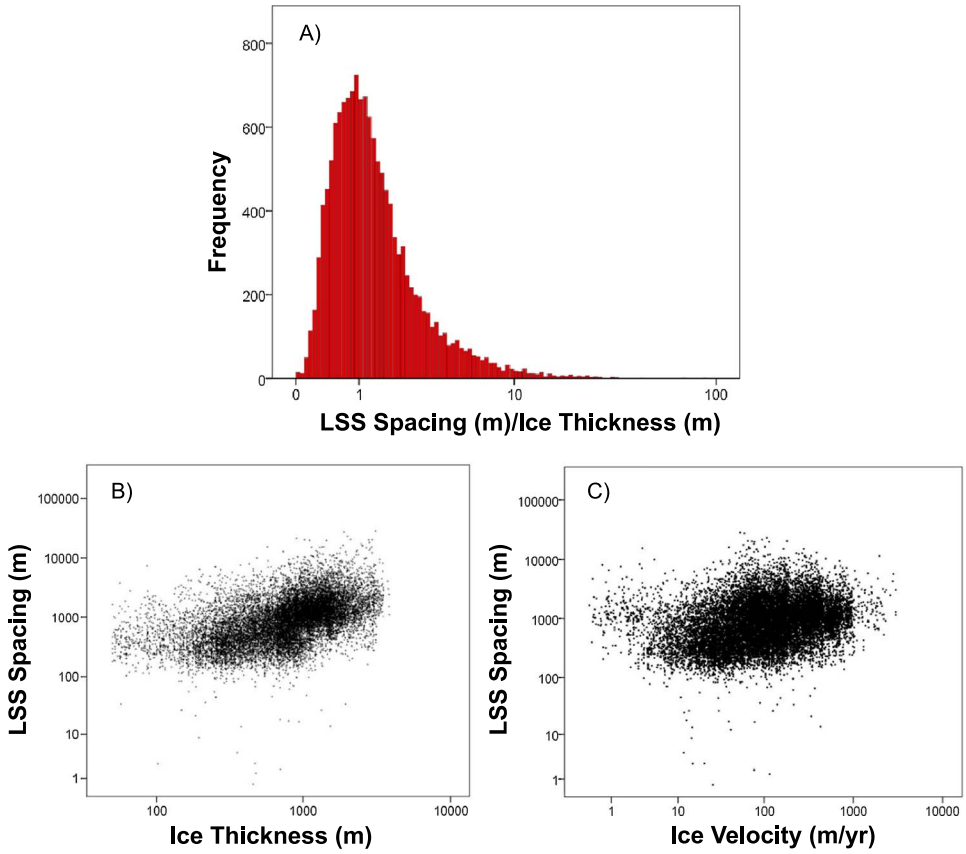

Figure 5. (a) The ratio of LSS spacing to ice thickness, showing a preference for LSSs to be spaced the same distance apart as the ice thickness. (b) The relationship between ice thickness and LSS spacing, which shows a weak positive relationship ($r^2 = 0.23$). (c) Conversely, no relationship ($r^2 = 0.01$) was found between LSS spacing and ice velocity. Note the logarithmic scales. In these cases, ice thickness was measured between LSSs.

Figures 3c and 3d show the distribution of ice flow velocities at the points where LSSs start. Nearly all (98%) LSSs begin at locations where ice velocities are below 700 m/yr, most (75%) below 120 m/yr, and some of them begin in regions flowing as slowly as <1 m/yr. Many of those observed in slower regions of ice flow occur toward the interior of the ice sheet, often starting at ice stream onsets. LSSs occur over a large range of ice thicknesses, between 50 m and 4000 m (Figures 3e and 3f), mostly centered at around 1000 m thickness with a positive skew to the distribution (Table 1). LSS spacing is frequently close to one ice thickness value, with the majority (60%) of LSSs spaced between 0.6 and 2.2 ice thicknesses apart (Figure 5). There is a slight tendency for LSSs on thicker ice to be spaced farther apart (Figure 5b), but we found no relationship between LSS spacing and ice velocity (Figure 5c).

Figure 3g shows that LSSs are observed to start in areas of converging, broadly parallel, and diverging ice flow (where planimetric convergence is respectively >0, ≈ 0, and < 0). While there is a tendency for their start points to occur on broadly parallel flow, LSS start points have a mean convergence value of 0.79 (Table 1), greater than the Antarctic wide mean of 0.012 [*Ng*, 2015], indicating that LSSs more commonly start in converging rather than diverging ice flow. This is reflected in the asymmetric distribution of Figure 3g. Furthermore, the measurements taken from the start point of LSSs are statistically different from values derived from a spatially random sample distributed across the grounded portion of Antarctica ($p < 0.05$). Figure 6 shows examples of LSSs beginning at areas of highly convergent flow. In these examples, LSSs are concentrated in regions of the ice which exhibit convergent (red on Figure 6) and broadly parallel (white on Figure 6) flow. Some of the strongest coincidences of LSS initiation and convergent flow include regions which are leeward of bed bumps as identified by *Ng* [2015]. Furthermore, Figure 6 demonstrates how LSSs show a tendency to avoid and/or terminate near regions of diverging ice (blue regions in Figure 6).

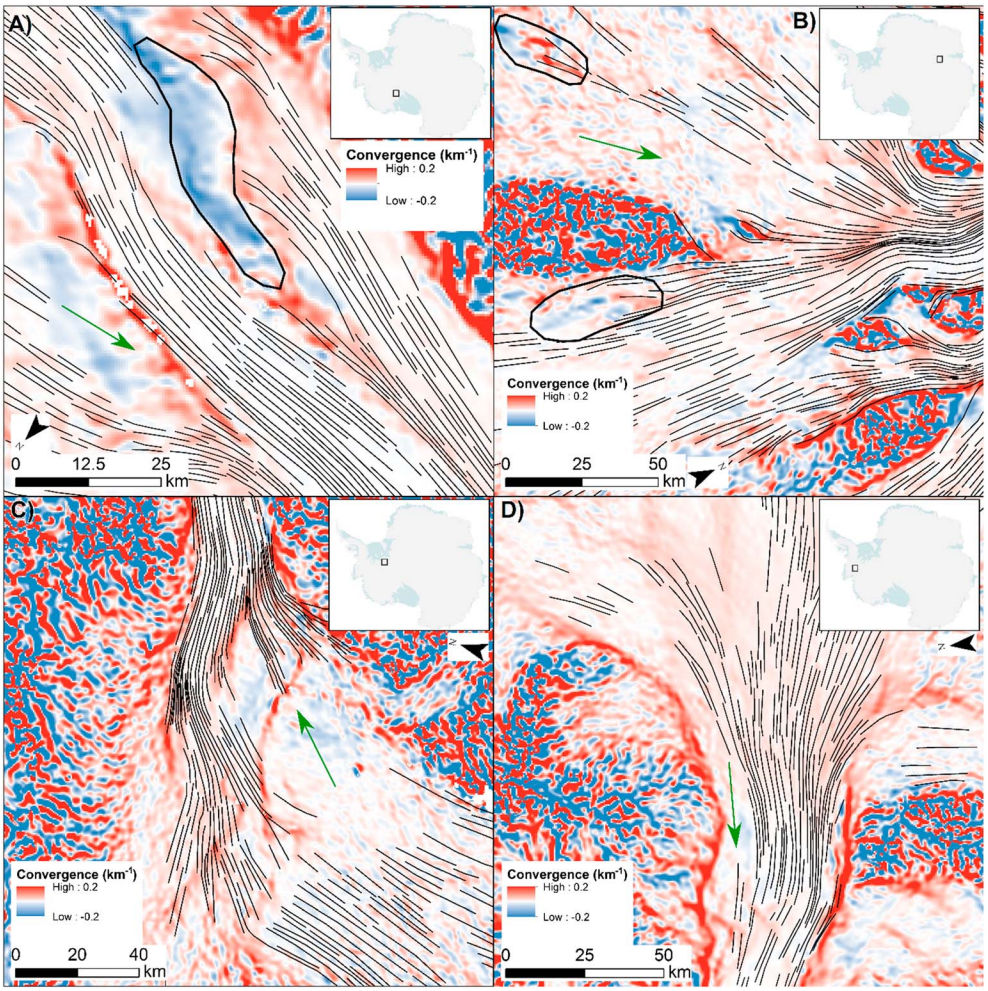

Figure 6. Comparison between LSS location (black lines) and planimetric flow convergence (background field in color scale) independently measured from ice velocity vectors [*Ng*, 2015]. (a) Binschadler ice stream. Note the lack of LSSs over areas of strong divergence (blue), in this case caused by bumps at the bed (identifiable from BEDMAP-2 data) highlighted in black [*Ng*, 2015]. (b) Mellor Glacier. LSSs formed in convergent flow zones on the downstream side of steps in bed topography, highlighted in black and noted by *Ng* [2015]. Further examples of a preference for LSSs to occur in converging ice flow are shown at (c) Foundation Ice Stream and (d) Pine Island Glacier. Green arrows denote general ice flow direction.

4. Discussion

A successful theory of LSS formation should be able to explain why LSSs have the morphological and glaciological properties presented above. Here we consider whether previously proposed mechanisms can account for the observed LSS characteristics.

Our mapping shows that most LSSs begin in converging or broadly parallel ice flow (Figure 3g and Table 1), and LSSs tend to avoid regions of divergent ice flow (e.g., Figure 6a). As ice convergence would cause ice to compress laterally and extend longitudinally, these characteristics are consistent with the hypothesis of LSS formation via lateral compression and longitudinal extension [e.g., *Reynolds and Hambrey*, 1988; *Hambrey and Glasser*, 2003; *Glasser et al*., 2015]. Furthermore, LSSs often appear sharply defined (likely due to a greater relief) at ice flow unit boundaries and more diffuse toward the center of a flow unit (e.g., Figure 7). Longitudinal foliations found on glaciers, thought to form by lateral compression and longitudinal extension, have also been reported to be more strongly developed at the lateral edges of flow units [e.g., *Allen et al*., 1960; *Hambrey and Müller*, 1978; *Hambrey et al*., 2005]. For the majority of flow units, the increased definition of LSSs is also combined with an increase in their spatial frequency. Often, the confluence of two flow units is marked by a depression, the formation of which is attributed to strong transverse convergence and

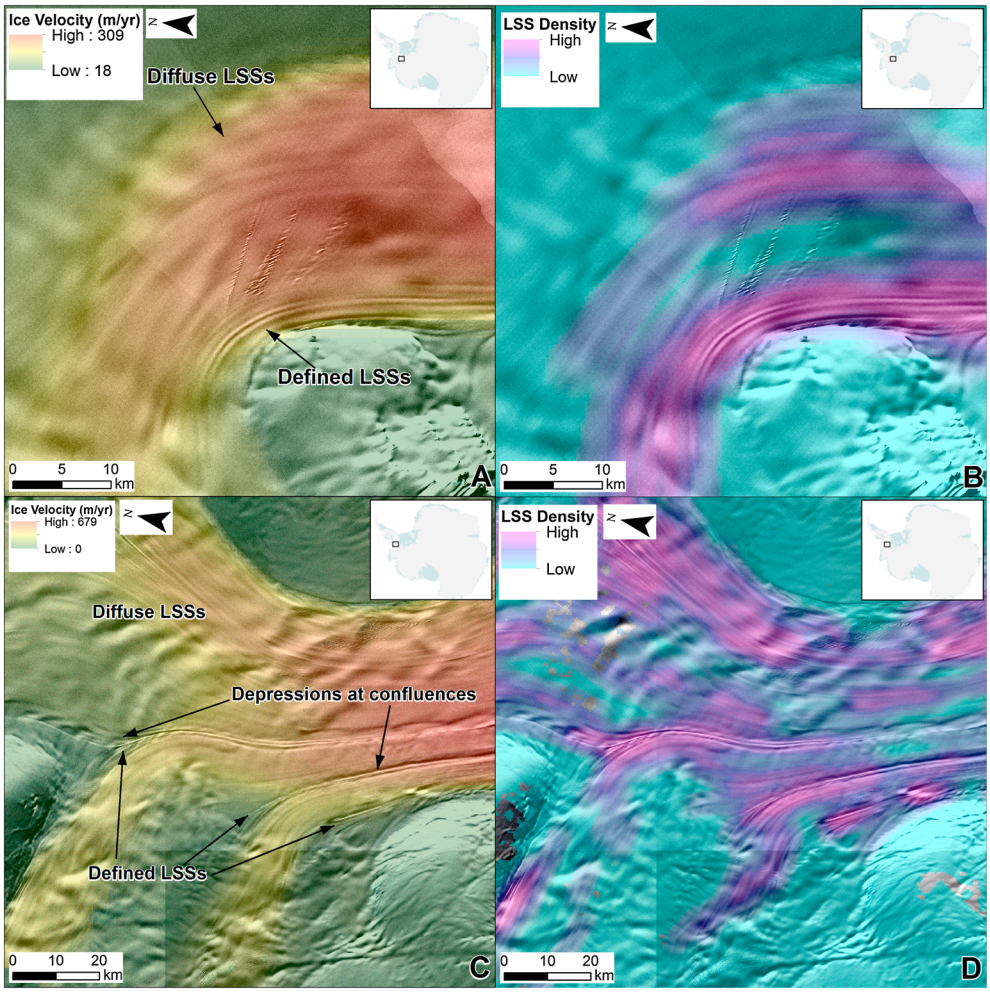

Figure 7. Landsat ETM+ images of LSSs with superimposed (left column) velocity and (right column) density data. (a) Pronounced LSSs at the edges of the Rutford Ice Stream. (b) Note how LSSs are diffuse in the main trunk but concentrated at the flow unit edge. (c) Several confluences at the Evans Ice Stream system. (d) Depressions form between flow units, and LSSs are concentrated at flow unit edges.

longitudinal extension [*Glasser and Gudmundsson*, 2012] (Figure 7c). The same stress regime likely explains the increased definition of LSSs at flow unit boundaries, lending further support to the lateral compression hypothesis. Indeed, *Ng* [2015] found that many ice stream tributary shear margins, which are often colocated with flow unit boundaries, exhibit strongly convergent flow (planimetric convergence >0). This, coupled with the differential flow velocities which occur at shear margins causing simple shear [*Glasser et al.*, 2015], means that shear margins may act as loci along which LSSs initiate, explaining why more LSSs are found near flow unit boundaries (e.g., Figure 7). LSS spacing is positively correlated with flow unit width (Figure 4). As shear margins dominate the stress imposed upon the ice [*Gudmundsson*, 2003], we interpret the change in LSS spacing with flow unit width as a response to changes in the stresses imposed upon the ice by the edges of the flow unit. In other words, flow unit narrowing causes lateral compression and longitudinal extension of ice; this creates new LSSs in the flow while causing existing LSSs to converge, and these two factors lead to a reduction in LSS spacing overall. Overall, many of the characteristics that we observe are consistent with LSS formation by lateral compression and longitudinal extension of ice, caused by the channeling of ice into an ice stream or outlet glacier.

The flow of rapidly sliding ice over a basal perturbation has also been thought to cause LSSs [*Gudmundsson et al.*, 1998]. Modeling shows that ice flow is laterally compressive and longitudinally extensional in the lee side of a bed perturbation (either a bed bump and/or a sticky spot) [*Gudmundsson*, 2003]. This modeling result is supported by observations of converging ice flow in the lee of steps in bed topography

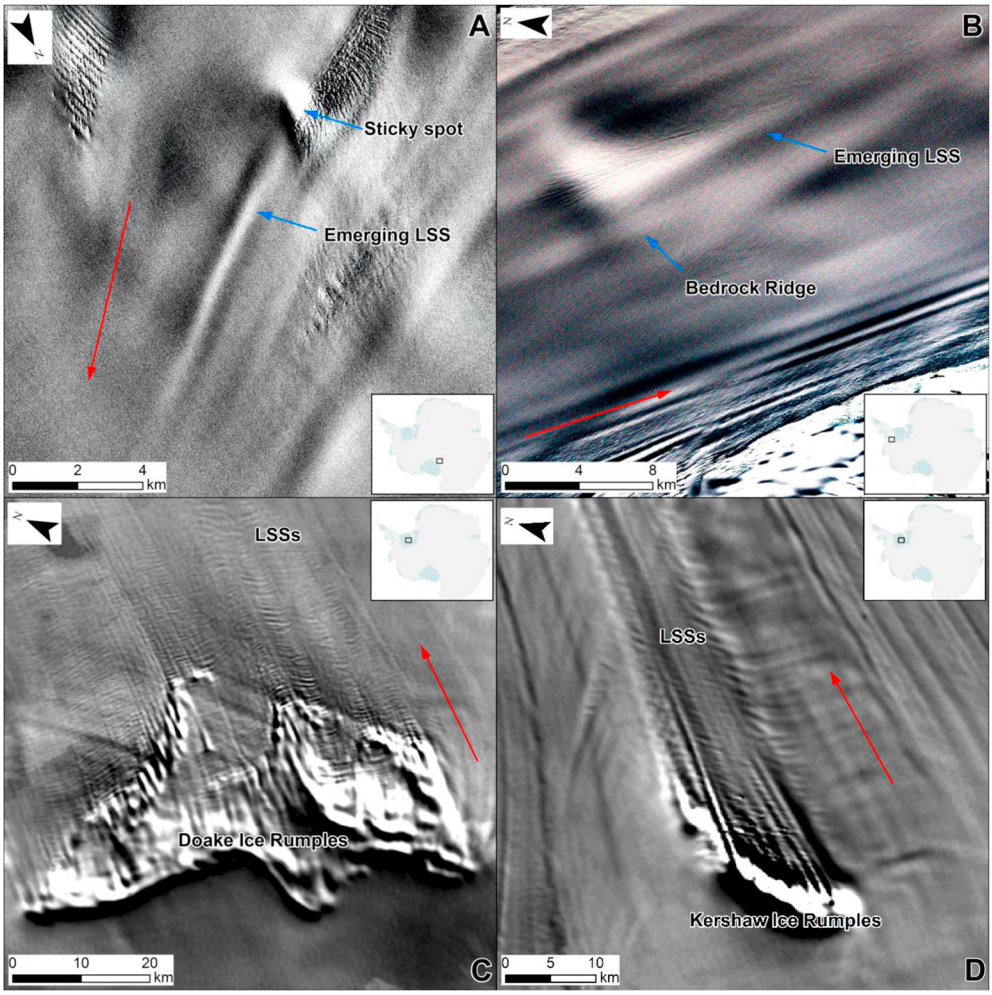

Figure 8. Examples of LSSs formed near changes to basal shear stress. (a) An LSS formed in the lee of a probable sticky spot on Byrd Glacier. (b) An LSS formed behind a bedrock ridge (described in *King et al*. [2016]), the Rutford Ice Stream. (c and d) examples of LSSs formed behind ice rumples on the Ronne Ice Shelf.

[*Ng*, 2015]. Here we indeed observe LSSs that initiate in the lee of topographic steps identified in the BEDMAP2 data (e.g., Figure 6b) and/or bumps in the ice surface likely caused by basal perturbations or sticky spots (Figures 8a and 8b) [*Stokes et al*., 2007]. LSSs were also noted to begin on ice rumples (Figure 8c and 8d), where the regrounding of the ice causes basal shear stress to increase to above the 0 value of the surrounding ice shelf. These examples highlight that some LSSs are likely the surface expressions of bed perturbations and are consistent with the basal transfer hypothesis [*Gudmundsson et al*., 1998]. These LSSs which are observed to initiate in the lee of basal perturbations (be they bumps or sticky spots) can also be viewed as a consequence of lateral compression and longitudinal extension.

Though LSSs associated with perturbations in the bed exist (e.g., Figures 6a, 6b, and 8), the basal transmission hypothesis is unable to account for the characteristics of all of the LSSs observed here. The formation of LSSs via the transmission of basal variability to the ice surface requires ice with a high ratio of sliding compared to internal ice deformation. Therefore, those LSSs beginning at ice stream onset zones at a sufficiently low sliding velocity (Figures 3c and 3d) [*Merry and Whillans*, 1993; *Hodge and Doppelhammer*, 1996] cannot be accounted for by the basal transfer hypothesis [*Gudmundsson et al*., 1998]. Possibly, these LSSs could have arisen from the increased shear strain occurring at the onset of ice streams [*Merry and Whillans*, 1993]. The acceleration of ice into an ice stream is accompanied by longitudinal extension, and lateral compression is likely there as many ice stream onsets display a convergent pattern [*Margold et al*., 2015]. Furthermore, if basal transmission were the cause of all LSSs and basal perturbations were evenly distributed across the

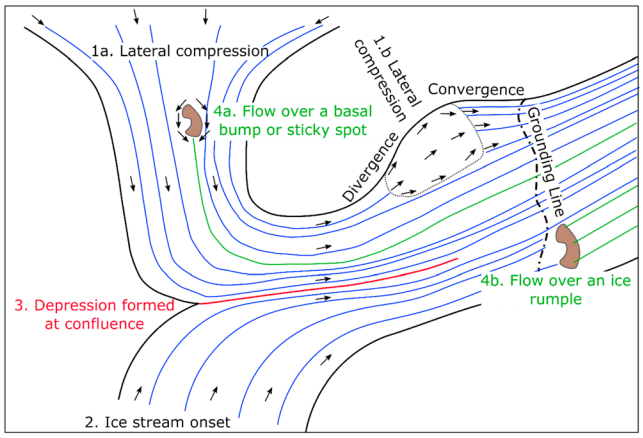

Figure 9. Conceptual model of LSS formation, as the consequence of increased strain in four different situations. Black lines denote flow unit boundary. (1) LSSs formed by lateral compression and longitudinal extension in two situations (blue). (1a) During convergence into a channel. (1b) Due to converging regions of ice within an ice stream, usually downstream of a region of diverging ice flow. (2) LSSs formed at the onset of fast ice flow. (3) Depressions (red) formed at the confluence of two ice channels, where ice flow also converges [*Glasser and Gudmundsson*, 2012; *Ng*, 2015]. (4) LSSs formed at variations in basal shear stress (green), either a sticky spot (4a) or an ice rumple (4b).

bed of Antarctica, then this mechanism would mean that LSSs would be more densely spaced on thinner and faster flowing ice. However, we found only a weak correlation between LSS spacing and ice thickness (Figure 5b) and no significant relationship between spacing and ice velocity (Figure 5c). This result is either a consequence of the fast ice flow preferentially occurring on smooth beds [e.g., *Siegert et al*., 2004] leading to a lack of basal bumps in areas of the ice sheet which are sliding to form LSSs or due to LSSs caused by other mechanisms. Given these considerations, and that the majority of LSS characteristics can be explained by the lateral compression and longitudinal extension of ice imposed by flow unit geometry, we suggest that LSSs caused by flow over bed perturbations are in the minority.

Given the above, we propose that LSSs are formed due to increased strain in regions of lateral compression and longitudinal extension, which occurs in four distinct instances (Figure 9):

1. The first is in areas of lateral compression and longitudinal extension imposed by ice flow geometry. This appears to be where the majority of LSSs appear to be formed. The lateral compression and longitudinal extension hypothesis accounts for many characteristics of LSSs, including their increased frequency and relief at flow unit boundaries (Figure 7), the positive correlation found between spacing and flow unit width (Figure 4), and their tendency to form in converging or parallel ice flow while avoiding diverging flow (Figures 3g and 6). Furthermore, it requires no specific ice thicknesses or velocities (Figures 3c–3f and 5).
2. The next is in ice stream onset zones, as demonstrated by observations of LSSs in these zones of low ice velocity (Figures 3c and 3d).
3. Another is at the convergence of two ice masses, where a separate type of LSS in the form of a depression is found [*Glasser and Gudmundsson*, 2012]. These are often surrounded by prominent LSSs (Figure 8).
4. And the last is in the convergent regions in the lee of abrupt changes in basal shear stress induced by sticky spots, bed bumps, or ice rumples, where increased ice strain promotes LSS development (e.g., Figures 6a, 6b, and 9).

Scenarios (1–4) of this conceptual model, which derives from our empirical observations, await detailed ice dynamical modeling investigations. The characteristics reported here act as tests for any model of LSS formation.

5. Summary and Conclusions

Analysis of the morphological and glaciological properties of LSSs shows that the majority of LSSs are spaced 450–1500 m apart and that this spacing has a strong positive correlation with flow unit width. LSSs occur at a wide range of ice thicknesses and can form where ice velocity is as low as ≈ 1 m/yr. The majority of LSSs form in converging ice and are more pronounced at flow unit confluences, where surface depressions form. We also note multiple instances where LSSs coincide with areas with nonuniform basal shear stresses (due to sticky spots, steps in bed topography. and ice rumples). From this, we propose that LSSs are formed due to increased strain experienced (i) during the lateral compression and longitudinal extension of ice into a channel, the most common scenario; (ii) at the onset to ice streaming; (iii) at flow unit confluence; and (iv) as ice flows over a basal perturbation.

Acknowledgments
J.C.E. would like to thank the Denisons for funding his PhD. Andrew Sole and Colm Ó'Cofaigh are also thanked for comments during J.C.E.'s PhD viva. We also thank the Editor Bryn Hubbard, Neil Glasser, and an anonymous reviewer for their constructive comments on this manuscript. Data related to this study can be obtained by contacting the lead author (j.ely@sheffield.ac.uk).

References

Allen, C. R., W. B. Kamb, M. F. Meier, and R. P. Sharp (1960), Structure of the lower blue glacier, Washington, *J. Geol.*, *68*(6), 601–625.
Burgess, D. O., M. J. Sharp, D. W. F. Mair, J. A. Dowdeswell, and T. J. Benham (2005), Flow dynamics and iceberg calving rates of Devon ice cap, Nunavut, Canada, *J. Glaciol.*, *51*(173), 219–230.
Casassa, G. (1991), Relict flow stripes on the Ross ice shelf, *Ann. Glaciol.*, *15*(1), 132–139.
Casassa, G., and I. M. Whillans (1994), Decay of surface topography on the Ross ice shelf, Antarctica, *Ann. Glaciol.*, *20*(1), 249–253.
Catania, G., C. Hulbe, H. Conway, T. A. Scambos, and C. F. Raymond (2012), Variability in the mass flux of the Ross ice streams, West Antarctica, over the last millennium, *J. Glaciol.*, *58*(210), 741–752.
Catania, G. A., H. Conway, C. F. Raymond, and T. A. Scambos (2005), Surface morphology and internal layer stratigraphy in the downstream end of Kamb ice stream, West Antarctica, *J. Glaciol.*, *51*(174), 423–431.
Conway, H., G. Catania, C. F. Raymond, A. M. Gades, T. A. Scambos, and H. Engelhardt (2002), Switch of flow direction in an Antarctic ice stream, *Nature*, *419*(6906), 465–467.
Crabtree, R. D., and C. S. M. Doake (1980), Flow lines on Antarctic ice shelves, *Polar Rec.*, *20*(124), 31–37.
Dowdeswell, J. A., and N. F. McIntyre (1987), The surface topography of large ice masses from Landsat imagery, *J. Glaciol.*, *33*(113), 16–23.
Ely, J. (2016), Flow signatures on the bed and the surface of ice sheets, PhD thesis, Univ. of Sheffield.
Ely, J. C., and C. D. Clark (2016), Flow-stripes and foliations of the Antarctic ice sheet, *J. Maps*, *12*(2), 249–259.
Fahnestock, M. A., T. A. Scambos, R. A. Bindschadler, and G. Kvaran (2000), A millennium of variable ice flow recorded by the Ross ice shelf, Antarctica, *J. Glaciol.*, *46*(155), 652–664.
Fretwell, P., et al. (2014), Bedmap2: Improved ice bed, surface and thickness datasets for Antarctica, *Cryosphere*, *7*, 375–393.
Glasser, N. F., and T. A. Scambos (2008), A structural glaciological analysis of the 2002 Larsen B ice-shelf collapse, *J. Glaciol.*, *54*(184), 3–16.
Glasser, N. F., and G. H. Gudmundsson (2012), Longitudinal surface structures (flowstripes) on Antarctic glaciers, *Cryosphere*, *6*(2), 383–391.
Glasser, N. F., S. Jennings, and M. J. Hambrey (2015), Origin and dynamic significance of longitudinal structures ("flow stripes") in the Antarctic ice sheet, *Earth Surf. Dyn.*, *3*(2), 239–249.
Gudmundsson, G. H., C. F. Raymond, and R. Bindschadler (1998), The origin and longevity of flow stripes on Antarctic ice streams, *Ann. Glaciol.*, *27*(1), 145–152.
Gudmundsson, G. H. (2003), Transmission of basal variability to a glacier surface, *J. Geophys. Res.*, *108*(B5), 2253, doi:10.1029/2002JB002107.
Hambrey, M. J., and N. F. Glasser (2003), The role of folding and foliation development in the genesis of medial moraines: Examples from Svalbard glaciers, *J. Geol.*, *111*(4), 471–485.
Hambrey, M. J., and A. G. Milnes (1977), Structural geology of an alpine glacier (Griesgletscher, Valais, Switzerland), *Eclogae Geol. Helv.*, *70*, 667–684.
Hambrey, M. J., and J. A. Dowdeswell (1994), Flow regime of the Lambert glacier-Amery ice shelf system, Antarctica: Structural evidence from Landsat imagery, *Ann. Glaciol.*, *20*(1), 401–406.
Hambrey, M. J., and F. Müller (1978), Structures and ice deformation in the white glacier, Axel Heiberg Island, northwest territories, Canada, *J. Glaciol.*, *20*(82), 41–66.
Hambrey, M. J., T. Murray, N. F. Glasser, A. Hubbard, B. Hubbard, G. Stuart, S. Hansen, and J. Kohler (2005), Structure and changing dynamics of a polythermal valley glacier on a centennial timescale: Midre Lovénbreen, Svalbard, *J. Geophys. Res.*, *110*, F01006, doi:10.1029/2004JF000128.
Hodge, S. M., and S. K. Doppelhammer (1996), Satellite imagery of the onset of streaming flow of ice streams C and D, West Antarctica, *J. Geophys. Res.*, *101*(C3), 6669–6677, doi:10.1029/95JC02961.
Jennings, S., M. J. Hambrey, and N. F. Glasser (2014), Ice flow-unit influence on glacier structure, debris entrainment and transport, *Earth Surf. Processes Landforms*, *39*(10), 1279–1292.
Jezek, K., X. Wu, J. Paden, and C. Leuschen (2013), Radar mapping of Isunnguata Sermia, Greenland, *J. Glaciol.*, *59*(218), 1135–1146.
Joughin, I., M. Fahnestock, R. Kwok, P. Gogineni, and C. Allen (1999), Ice flow of Humboldt, Petermann and Ryder Gletscher, northern Greenland, *J. Glaciol.*, *45*(150), 231–241.
King, E. C., H. D. Pritchard, and A. M. Smith (2016), Subglacial landforms beneath Rutford Ice Stream, Antarctica: Detailed bed topography from ice-penetrating radar, *Earth Syst. Sci. Data*, *8*(1), 151–158.
Margold, M., C. R. Stokes, and C. D. Clark (2015), Ice streams in the Laurentide ice sheet: Identification, characteristics and comparison to modern ice sheets, *Earth Sci. Rev.*, *143*, 117–146.
Mayer, H., and U. C. Herzfeld (2000), Structural glaciology of the fast-moving Jakobshavn Isbræ, Greenland, compared to the surging Bering glacier, Alaska, USA, *Ann. Glaciol.*, *30*(1), 243–249.
Merry, C. J., and I. M. Whillans (1993), Ice-flow features on ice stream B, Antarctica, revealed by SPOT HRV imagery, *J. Glaciol.*, *39*(133), 515–527.
Ng, F. S. L. (2015), Spatial complexity of ice flow across the Antarctic ice sheet, *Nat. Geosci.*, *8*(11), 847–850.
Raup, B. H., T. A. Scambos, and T. Haran (2005), Topography of streaklines on an Antarctic ice shelf from photoclinometry applied to a single advanced land imager (ALI) image, *IEEE Trans. Geosci. Remote Sens.*, *43*(4), 736–742.
Reynolds, J. M., and M. J. Hambrey (1988), The structural glaciology of George VI ice shelf, Antarctic peninsula, *Bull. British Antarc. Surv.*, *79*, 79–95.
Rignot, E., J. Mouginot, and B. Scheuchl (2011), Ice flow of the Antarctic ice sheet, *Science*, *333*(6048), 1427–1430.
Siegert, M. J., J. Taylor, A. J. Payne, and B. Hubbard (2004), Macro-scale bed roughness of the Siple coast ice streams in West Antarctica, *Earth Surf. Processes Landforms*, *29*(13), 1591–1596.
Siegert, M., N. Ross, H. Corr, J. Kingslake, and R. Hindmarsh (2013), Late Holocene ice-flow reconfiguration in the Weddell Sea sector of West Antarctica, *Quat. Sci. Rev.*, *78*, 98–107.
Spagnolo, M., C. D. Clark, J. C. Ely, C. R. Stokes, J. B. Anderson, K. Andreassen, A. G. C. Graham, and E. C. King (2014), Size, shape and spatial arrangement of mega-scale glacial lineations from a large and diverse dataset, *Earth Surf. Processes Landforms*, *39*(11), 1432–1448.
Stokes, C. R., C. D. Clark, O. B. Lian, and S. Tulaczyk (2007), Ice stream sticky spots: A review of their identification and influence beneath contemporary and palaeo-ice streams, *Earth Sci. Rev.*, *81*(3–4), 217–249.
Swithinbank, C., and B. K. Lucchitta (1986), Multispectral digital image mapping of Antarctic ice features, *Ann. Glaciol.*, *8*(1), 159–163.
Swithinbank, C., K. Brunk, and J. Sievers (1988), A glaciological map of Filchner-Ronne ice shelf, Antarctica, *Ann. Glaciol.*, *11*, 150–155.
Vornberger, P. L., and I. M. Whillans (1986), Surface features of Ice Stream B, Mair Byrd Land, West Antarctica, *Ann. Glaciol.*, *8*(1), 168–170.
Wyatt, F. R., and M. J. Sharp (2015), Linking surface hydrology to flow regimes and patterns of velocity variability on Devon ice cap, Nunavut, *J. Glaciol.*, *61*(226), 387–399.